Design of Post-Tensioned Girder Anchorage Zones

William C. Stone
Research Structural Engineer
Center for Building Technology
National Bureau of Standards
Washington, D.C.

John E. Breen*
The Carol Cockrell Curran
Chair in Engineering
Department of Civil Engineering
The University of Texas
Austin, Texas

Synopsis

The post-tensioned anchorage zones of several thin-webbed box girders, which were designed in accordance with AASHTO and ACI requirements, have cracked along the tendon path during stressing. This cracking presents paths for potential corrosion and frost damage. In addition, such cracking negates a major benefit of prestressed concrete, namely, the minimization of service load cracking.

This report summarizes the major design-related observations and conclusions from an extensive analytical and experimental study of the behavior of post-tensioned anchorage zones with single large tendons. The experimental program considered variables such as tendon inclination and eccentricity, anchor width and geometry, and the effect of supplementary anchorage zone reinforcement. Three-dimensional computer analyses were used to generalize these results. A failure theory developed to explain tendon path crack initiation agreed well with the experimental data.

A general equation for cracking load in specimens without supplemental anchorage zone reinforcement is presented along with provisions for designing supplementary reinforcement and calculating the effect it will have on cracking and ultimate load. Suggested code and commentary changes, based on the results of the above mentioned data, are presented. Examples showing practical applications of the tentative recommendations are included.

Table 1. Regression Analysis Data.

Case	Specimen	P_{cr} (kips)	t (in.)	$2a'$ (in.)	f_{sp} (ksi)	$2a$ (in.)	e (in.)	θ (deg)
1	MR1A	39	3	2.625	0.723	20.5	0	0
2	MR1B	43	3	2.125	0.725	20.5	0	0
3	MI1B	41	3	2.125	0.697	20.5	0	0
4	MI2	30	3	2.625	0.582	20.5	0	30
5	FS1A	400	12	8.5	0.451	82	0	0
6	FS1B	400	12	10.5	0.401	82	0	0
7	FS2B	330	12	10.5	0.455	82	0	30
8	M7A-4	15	3	2	0.327	20	3	0
9	M7C-4	32	3	2	0.548	20	3	0
10	M1A-4	31	3	2	0.495	20	6	0
11	M8B-4	31	3	2	0.707	20	6	0
12	M1-2	43	4	2	0.627	20	0	0
13	M2-2	34	3	2	0.627	20	0	0
14	M3-2	24	2	2	0.627	20	0	0
15	M3-2R	18	2	2	0.460	20	0	0
16	M2A-4	18	3	2	0.495	20	6	0
18	FS2A	440	12	10.5	0.532	82	0	15
19	M1-3	28	3	2	0.610	20	0	30
20	M2-3	32	4.5	2	0.637	20	0	30

Note: 1 kip = 4.45 kN; 1 in. = 25.4 mm; 1 ksi = 6.9 MPa.

This paper is the second in a two-part series summarizing a study performed at the University of Texas at Austin on the behavior of post-tensioned girder anchorage zones. In the first paper[1] a summary of the major behavioral observations and conclusions from an extensive analytical and experimental program[2,3] was presented.

The experimental program investigated the primary variables affecting the formation of the tendon path crack: tendon inclination and eccentricity, section height and width, tensile splitting strength of the concrete, anchor width and geometry, and the effect of supplementary anchorage zone reinforcement, both active and passive. An extensive series of three-dimensional linear elastic finite element computer analyses was used to generalize these results and develop a failure theory to explain tendon path crack initiation based upon specified peak spalling strains at the edge of the anchorage.

In this paper specific methods of predicting cracking and ultimate loads are presented based on a comprehensive regression analysis of the test data and on the indications of the three-dimensional finite element method analyses.[4] A limit state design philosophy with appropriate factors of safety for cracking and ultimate loads is presented.

There are two general approaches available for the design of post-tensioned anchorage zone reinforcement. These are:

1. To design the section geometry and supplementary anchorage zone reinforcement so that cracking will not occur at maximum stressing load levels.

2. To allow anchorage zone cracking to occur during stressing but to provide

*Also, Director, Phil M. Ferguson Structural Engineering Laboratory, University of Texas. Currently, Chairman, ACI Committee 318, Building Code Requirements for Reinforced Concrete. Recipient of PCI's State-of-the-Art Award in 1981 (paper published in Jan.-Feb. 1980 PCI JOURNAL).

proper reinforcement so that crack widths at the stressing load will not exceed an allowable value selected to minimize the possibility of water penetration and corrosion.

In either case the anchorage ultimate load capacity must be kept well above the cracking load to ensure adequate safety and to give warning of structural distress.

CRACKING LOAD PREDICTION

In the earlier paper[1] and detailed report[3] an extensive series of physical tests of thin web anchorage zones was reported. A step-wise linear regression analysis considering all geometric variables in the test program was performed using the results[3] of the 20 tests for which no supplementary anchorage zone reinforcement was provided. Both model and full-scale data were included as shown in Table 1.

Variables with low statistical meaning were gradually eliminated. The resulting empirically based general cracking equation for thin web members is expressed as a function of six key variables. Elimination of any of these variables made major and undesirable changes in the correlation.

The resulting expression with slight modifications to simplify terms is:

$$P_{cr_{(plate)}} = t\left[\frac{f_{sp}}{24}(38a - 120) - \frac{t}{81}\{2\theta - 252\,(e/a)\,f_{sp}\} - \frac{103}{9}(e/a) - 7\right] + 39a' + \frac{f_{sp}}{5}\{166 - 975\,(a'/t)^2\} - 9.1 \qquad (1)$$

where, as shown in Fig. 1:

- e = tendon eccentricity (always assumed positive), in.
- $2a$ = section height, in.
- $2a'$ = width of anchor plate (assumed square), in.
- t = section thickness, in.
- θ = angle of tendon inclination (always assumed positive), deg
- f_{sp} = split cylinder tensile strength, ksi (may be conservatively estimated in psi units as $6.5\sqrt{f'_c}$)
- $P_{cr_{(plate)}}$ = cracking load for section with plate anchor, but without supplementary anchorage reinforcement, kips

To demonstrate the accuracy of Eq. (1), Table 2 compares the measured experimental cracking load against the calculated value. The mean of P_{cr} (test)/P_{cr} (calculated) was 1.004 with a standard deviation of 0.072. As an external check, Eq. (1) was used to calculate the expected cracking for a number of physical specimen tests performed by Cooper[5] and Berezovytch.[6] The results are shown in Table 3.

For the 16 comparisons made of these independent tests, the mean value of P_{cr} (test)/P_{cr} (calculated) was 1.127, indicating a moderate conservatism in the calculated values. The standard deviation was 0.23, which is high but not unreasonable given the expected scatter for tests which depend heavily on the tensile strength of concrete specimens.

Eq. (1) was developed from the test results for bearing or plate-type anchors. The results need to be modified for "bell" and "cone" type anchors. The three anchor types are shown in Fig. 4 of Ref. 1. The "cone" type anchor has stiff bearing walls in the conical section. A thin-walled transition trumpet on a plate anchor would not be classed as a "cone" type anchor. Test results reported in Ref. 3 indicate the following factors are appropriate:

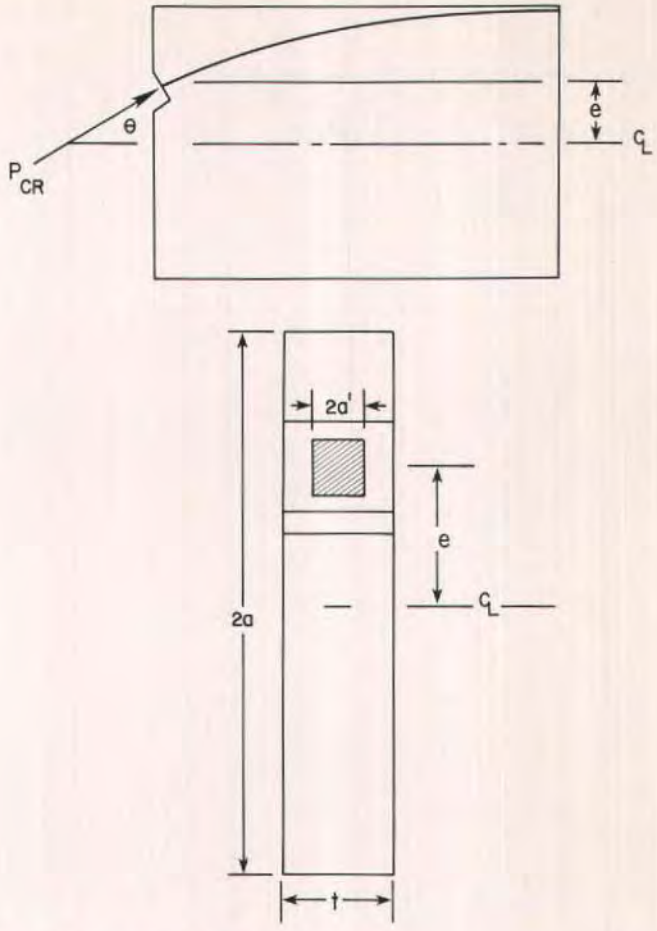

Fig. 1. Geometric data for Eq. (1)

Plate:

$$P_{cr} = 1.00\, P_{cr\,(plate)} \qquad (2a)$$

Bell:

$$P_{cr} = 1.08\, P_{cr\,(plate)} \qquad (2b)$$

Cone:

$$P_{cr} = 0.61\, P_{cr\,(plate)} \qquad (2c)$$

LIMITATIONS

Eqs. (1) and (2), although intended for general applications, are empirical equations and hence have certain restrictions due to lack of data in some areas. They are appropriate for specimens and applications similar to the thin rectangular sections tested. Since the units on all terms are not physically consistent, the constants contain dimensionally related values. Hence, Eq. (1) must be used in the customary unit system. In addition, some other restrictions include:

1. Inclinations in the test program were always positive, as were eccentricities (see Fig. 1). Any combination of negative tendon eccentricity (i.e., below the centroid rather than above it) with

Table 2. Regression Analysis Results — Comparison of Predicted and Actual Cracking Loads.

Case	Specimen	P_{cr} (test) (kips)	P_{cr} [Eq. (1)] (kips)	$\frac{P_{cr}\text{ (test)}}{P_{cr}\text{ [Eq. (1)]}}$
1	MR1A	39	42.5	0.9176
2	MR1B	43	42.2	1.0189
3	MI1B	41	41.0	1.0
4	MI2	30	31.7	0.9464
5	FS1A	400	400.9	0.998
6	FS1B	400	398.4	1.004
7	FS2B	330	330.35	0.999
8	M7A-4	15	15.8	0.949
9	M7C-4	32	27.5	1.163
10	M1A-4	18	18.5	0.973
11	M8B-4	31	31.4	0.9873
12	M1-2	43	42.2	1.016
13	M2-2	34	36.6	0.929
14	M3-2	24	19.85	1.21
15	M3-2R	18	18.8	0.958
16	M2A-4	22	22.1	0.995
17	M1A-4	18	18.5	0.973
18	FS2A	440	438.8	1.0027
19	M1-3	28	29.1	0.962
20	M2-3	32	29.6	1.081

$\bar{X} = 1.0041$; $\sigma = 0.072$

positive tendon inclination or vice versa is not directly covered. It is likely that in such cases the tendon path crack would form at a higher load than when both inclination and eccentricity are positive. By using absolute values for angles and eccentricities, Eq. (1) should yield conservative solutions for such problems. This has not been verified experimentally.

2. Thin prismatic web sections are assumed. The limits of the experimental and computer data are for

$$0.05 \leq t/2a \leq 0.25.$$

3. Multiple tendons anchored in the same web section are not covered. Limited experimental evidence[3] indicates further conservatism is warranted for that case.

4. The anchorage is assumed to be square. Until further test data are available, the shorter edge distance should be used for $2a'$ when rectangular anchors are used (see Fig. 2d).

Although not specifically tested in this study, several practical applications should be soluble using Eqs. (1) and (2), and proper consideration of the geometry. These are:

(a) Laterally eccentric anchors and edge anchors, particularly in thick web sections.

(b) Multiple anchors across thick web sections.

(c) Rectangular anchor plates oriented such that $2a' < 2b'$.

These cases are illustrated in Fig. 2. Figs. 2a through 2c indicate that a conservative solution should be obtained by replacing the value t in Eq. (1) with the value $2g$ which equals twice the edge distance or the distance between the anchors. Strip type rectangular anchors such as shown in Fig. 2e where $2b' < 2a'$ cannot be accurately handled by Eq. (1) without further experimental or analytical investigation. However, rectangular anchors, such as shown in Fig. 2d

Table 3. External Check of Eq. (1).

Ref.	Specimen	P_{cr} (kips)	f'_c (psi)	f_{sp} (ksi)	t (in.)	$2a$ (in.)	θ (deg)	e (in.)	$2a'$ (in.)	Eq. (1) P_{cr} (kips)	$\frac{P_{cr}\text{ (test)}}{P_{cr}\text{[Eq. (1)]}}$
Cooper[5]	Spiral Reinf. No. 1, Set 3	12.6	7480	0.707	1.67	16	28	1.5	1.42	11.52†,‡	1.09
	Spiral Reinf. No. 1, Set 4	12.1	5550	0.595	1.67	16	28	1.5	1.42	10.11†,‡	1.19
	LPT Reinf. No. 1, Set 10	19.6	6830	0.661	1.67	16	28	1.5	1.42	16.76†,‡	1.16
Berezovytch[6]	II-1	37	3160	0.365	3	36	0	0	2	38.96	0.949
	II-2	36	3850	0.403	3	36	0	0	2	33	1.09
	II-3	40	3850	0.403	5	36	0	0	2	52	0.78
	II-4	44	3850	0.403	5	36	0	0	2	52	0.846
	III-1	40	2860	0.347	5	36	0	0	2	45	1.34
	III-2	54.5	2860	0.347	5	36	0	0	2	45	1.21
	III-4	40	2860	0.347	3	36	0	0	2	38	1.05
	III-5	75	4470	0.434	5	36	0	0	2	57	1.31
	III-6	100	4470	0.434	7	36	0	0	2	66	1.51
	III-8	107	4315	0.426	7	36	0	0	2	64	1.6
	IV-1	32	2460	0.323	3	36	0	0	2	35.4	0.904
	IV-2	55	3535	0.386	5	36	0	0	2	50.2	1.09

*f_{sp} for Cooper's test[5] estimated at $8\sqrt{f'_c}$; $6.5\sqrt{f'_c}$ for Berezovytch's tests.[6]
†Anchor laterally eccentric web. Effective thickness used (as shown in Fig. 2).
‡Modified to account for reinforcement.

$\bar{X} = 1.127$
$\sigma = 0.23$

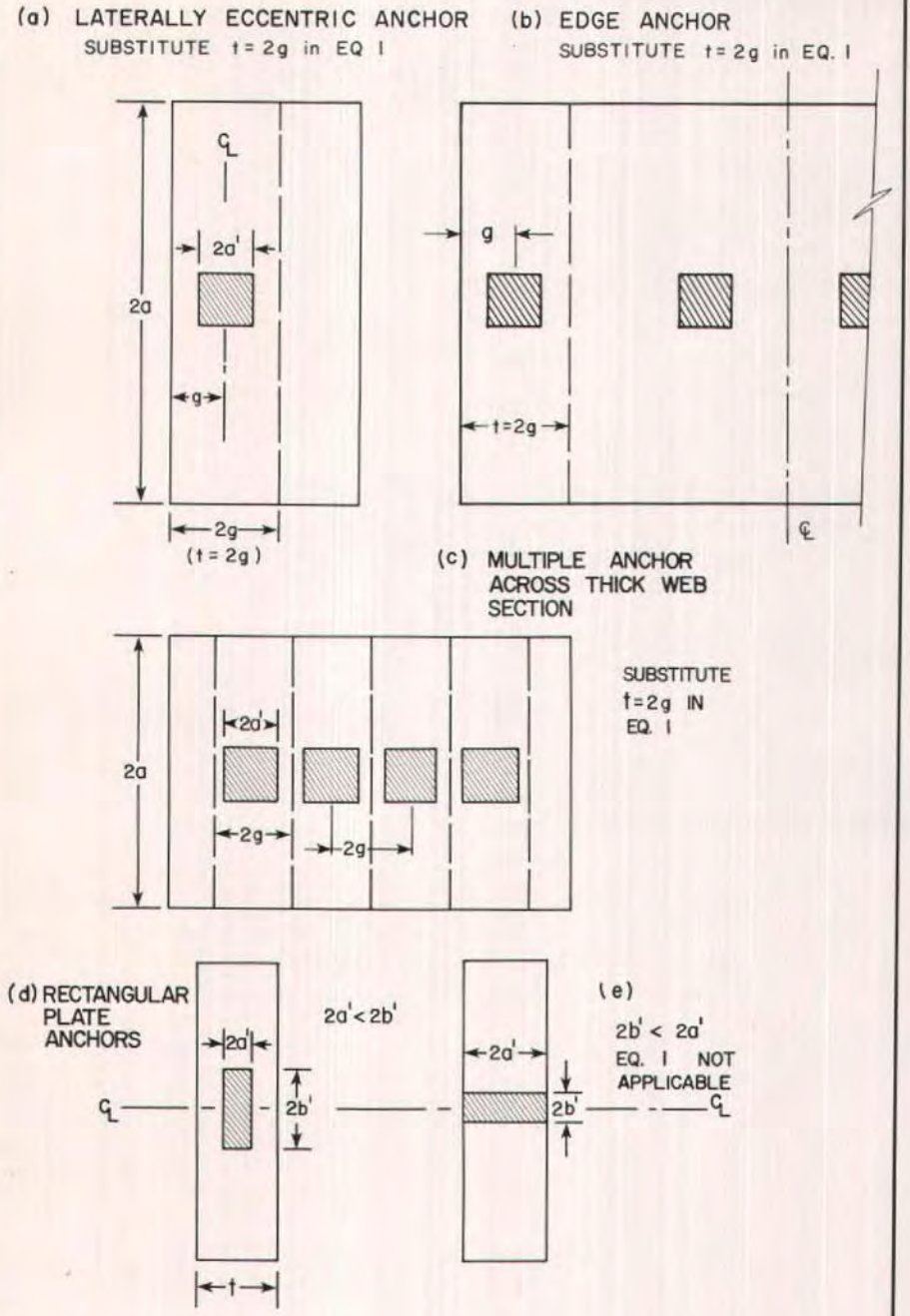

Fig. 2. Special cases for Eq. (1).

where $2a' < 2b'$, should be conservatively designed using Eq. (1).

For other complex applications, a more exact solution should be obtained using a linear elastic, three-dimensional finite element analysis,[2] or by further experimental investigation.

EFFECT OF SUPPLEMENTARY REINFORCEMENT

Cracking loads calculated from Eqs. (1) and (2) represent the minimum value to be expected for a normally reinforced section without supplementary anchorage zone reinforcement. A substantial number of tests dealing with various supplementary reinforcing methods indicated that cracking loads could be raised significantly by the addition of such reinforcement (passive or active). The expected rise in cracking load for a given type of reinforcement was presented in Refs. 3, 4, and 1.

Using these percentage increases and assuming a linear variation between the values for straight and inclined tendons, the cracking load for the reinforced anchorage zone with supplementary reinforcement is given by:

Spiral reinforcement:

$$P'_{cr} = (2.03 - 0.032\theta)\,P_{cr} \qquad (3a)$$

Orthogonal reinforcement:

$$P'_{cr} = (1.61 - 0.019\theta)\,P_{cr} \qquad (3b)$$

Active reinforcement
(Lateral post-tensioning):

$$P'_{cr} = (2.37 - 0.0372\theta)\,P_{cr} \qquad (3c)$$

where

P'_{cr} = predicted cracking load with supplemental reinforcement, kips
θ = angle of tendon inclination, deg
P_{cr} = cracking load for section with no supplementary reinforcement as calculated from Eqs. (1) and (2)

These equations are valid only for reinforcement amounts and locations designed in accordance with the provisions presented later in this paper.

ULTIMATE STRENGTH PREDICTION

A review of the ultimate load data for specimens without supplemental anchorage zone reinforcement shows a considerable amount of scatter. Some inclined tendon models developed ultimate loads 60 percent above cracking. Most (particularly among the straight tendon tests) exhibited very brittle behavior with an explosive failure of the anchorage zone occurring at a load coincident with or only slightly above that which caused formation of the tendon path crack.

For this reason the ultimate load for an anchor with no supplementary reinforcement should conservatively be equated with the cracking load. The ultimate load, however, is substantially increased for sections containing adequate supplementary reinforcement in the anchorage zone (active or passive), thus providing a desirable margin of safety between cracking and ultimate load. The relative increase in the ultimate load for a given supplementary anchorage zone reinforcing method was presented in Ref. 4.

Again, assuming a linear variation between the straight and inclined values from Ref. 4, the ultimate load for a given situation can be calculated as:

Spiral reinforcement:

$$P_{ult} = (3.18 - 0.53\theta)\,P_{cr} \qquad (4a)$$

Orthogonal reinforcement:

$$P_{ult} = (1.71 - 0.17\theta)\,P_{cr} \qquad (4b)$$

Active reinforcement:

$$P_{ult} = (3.89 - 0.046\theta)\,P_{cr} \qquad (4c)$$

where

P_{ult} = ultimate load with supplemental reinforcement, kips

θ = angle of tendon inclination, deg

P_{cr} = cracking load for section with no supplementary reinforcement as calculated from Eqs. (1) and (2), kips

These equations are valid only for reinforcement amounts and locations designed in accordance with the provisions presented later.

LIMIT STATE DESIGN

In general, when a structure or structural element becomes unfit for its intended use, it is said to have reached a limit state.[7] Limit state design is a design process which involves identification of all possible modes of failure (limit states), determination of an acceptable level of safety against occurrence of each limit state and consideration by the designer of the significant limit states. Limit states for the post-tensioned anchorage zone fall into two basic groups:

1. Ultimate limit states which are related to the structural collapse of part or all of the structure. Such a limit state should have a low probability of occurrence since it may lead to loss of life and major financial losses. Ultimate limit state for the post-tensioned anchorage zone would be evidenced by:

   (a) Explosive rupture of the anchorage zone.
   (b) Complete side face blow-out of a multiple strand curved tendon at the point of maximum curvature.

2. Damage limit states which are related to damage of the structure in the form of premature or excessively wide cracks. For the post-tensioned anchorage zone the damage limit state falls into two categories:

   (a) If the environment is a hostile one (corrosion and freeze-thaw damage possibilities), formation of any tendon path crack would constitute a damage limit state.
   (b) If the environment is nonhostile and minor cracking can be tolerated, the limit state would constitute the load at which crack widths became excessive [greater than about 0.012 to 0.013 in. (0.3 to 0.33 mm) as currently implicitly specified].

Since there is less danger of loss of life in the second group, a higher probability of occurrence can be tolerated than in the case of the ultimate limit state.

The design philosophy for these two limit states is to arrive at a best estimate of the highest load that will come into the structure with respect to a particular limit state. This load is then multiplied by an appropriate load factor which takes into account possibilities of overload, in addition to anticipated variations in the maximum load due to material tolerances.

This new load (with safety factor included) must be less than the best estimate of the nominal resistance of the structure to a particular limit state multiplied by a strength reduction factor (ϕ factor) which takes into account both the undesirability of a particular type of failure, as well as the possibility of material and construction defects (for example, substandard concrete).

Expressed in equation form:

$$(P_{LS})\,(\mathrm{LF}) \leq \phi P_{nom_{LS}} \qquad (5)$$

where

P_{LS} = best estimate of highest load to come onto structure at a particular limit state

$P_{nom_{LS}}$ = best estimate of nominal strength of structure with respect to a particular limit state

LF = load factor representing a factor of safety against reaching a particular limit state

ϕ = strength reduction factor which accounts for material and construction defects and undesirability of a particular limit state

LIMIT STATE DESIGN FOR CRACKING

Under the ACI Building Code the maximum permissible specified temporary prestressing load to be applied to any structure is $0.8f_{pu}$, that is to say, 80 percent of the guaranteed ultimate tensile strength of the prestressing tendon. Thus $P = 0.8f_{pu}A_{ps}$, where A_{ps} is the nominal area of the tendon.

In practice, a 10 percent overload could occur due to a jacking error such as miscalibration, misreading or overpumping. A 15 percent margin for error above that would constitute a reasonable factor of safety against a damage limit state. Thus, the total load factor recommended is equal to 1.25.

On the other side of the inequality is the cracking load derived from Eqs. (1) and (2) with appropriate modification to account for tendon geometry and supplemental reinforcement. Since Eq. (1) was selected as a lower bound prediction, the variance is relatively low, and since quality control is fairly good for prestressed concrete construction, a ϕ factor of 0.90 is reasonable. Thus:

$$P_{nom_{cr}} \geq \frac{(P_{cr})\,(\mathrm{LF})}{\phi} \geq \frac{(1.25)\,(0.8f_{pu})\,(A_{ps})}{0.90} = 1.10f_{pu}A_{ps} \quad (6)$$

Note that the application of consistent limit states procedure requires the anchorage zone to be designed so cracking would not occur at a load less than the tendon ultimate. This may appear extremely conservative but in reality, with the large number of possible factors which can lower the cracking load, this is a minimal requirement.

LIMIT STATE DESIGN FOR ULTIMATE

In general considerations of ultimate loading which may come on a structure, there is no practical bound on the upper limit of the load due to misloading. With prestressing forces, the tensile strength of the tendon imposes a practical upper bound. For the ultimate limit state, the nominal maximum stressing load on the structure would be the nominal ultimate capacity of the tendon ($1.0f_{pu}A_{ps}$). However, this is not the best estimate of the highest load which could come onto the structure.

Mill reports and metallurgist recommendations indicate that the actual steel area for a given tendon could be as much as 2.4 percent above the nominally specified cross-sectional area. Likewise, prestressing steel with a nominally specified ultimate strength of 270 ksi (1863 MPa) may reach 300 ksi (2070 MPa) maximum, representing an 11 percent rise in strength. Both of these values constitute upper bound limits, ones highly unlikely to occur simultaneously for all tendons in practice.

An additional consideration, hard to quantify, is the possibility of a greater number of strands being used than the number specified. This chance seems more remote but has been known to occur.

An appropriate load factor which would account for these effects at ultimate would be about 1.20. This is the value used by CEB-FIP for tendon force. Given the same material and construction quality as before, the capacity reduction factor for ultimate failure should be lower than for cracking, as an explosive anchorage failure may have a disastrous effect on the integrity of the overall structure. For this brittle-type failure, a value of $\phi = 0.75$, similar to that used for spiral columns, is recommended.

The design check for ultimate is thus:

$$P_{nom_{ult}} \geq \frac{(1.2)\,f_{pu}A_{ps}}{0.75} = 1.60f_{pu}A_{ps} \quad (7)$$

In the case of bonded tendons, the force at the anchorage is less likely to

increase once stressing is completed. A higher value of ϕ would be justified but the further complexity introduced makes such refinement questionable.

APPLICATION OF LIMIT STATE PHILOSOPHY

It is anticipated that the application of a reasonable limit state philosophy to post-tensioned anchorage zones will be a controversial subject. A cracking criterion based on a design tendon force of $1.10 f_{pu} A_{ps}$, as suggested above, at first glance seems wildly conservative in an industry which takes pride in "load testing" every structure during the post-tensioning process. Yet it is just this load testing that makes the requirement so important.

Almost every tendon is loaded to approximately $0.8 f_{pu} A_{ps}$ during jacking. With errors in ram calibration, pressure gauges, and human fallibility, certainly some are loaded beyond that point and probably more than 10 percent beyond. The remaining difference is the margin of safety which must not only account for possible dimensional errors, material understrengths and constructional deficiencies like honeycombing, but must provide for the wide variability associated with the imprecision of our knowledge and the general variability of concrete tensile properties.

It is even more important to focus on the ultimate state. The tendon can be called on to develop its full tensile capacity if the structure is overloaded. This tensile capacity is not the guaranteed minimum tensile strength but the actual tensile strength, based on actual (not nominal) area and actual tensile properties. The failure of an anchorage may be sudden, explosive, and devastating. A suitable reserve should be provided. The values suggested are actually less than are accepted for a ductile beam failure because of the higher confidence in the level of load.

Traditionally, in the United States a consistent design philosophy has not been applied to the anchorage zone. These load levels seem high when compared to what have been used. In the CEB-FIP criteria they have been more realistic. They require a load factor on prestress forces of 1.2 and resistance factors on concrete in the anchorage zone of 1.5. Thus, the comparable ultimate load when adjusted for variations in concrete quality control would be equivalent to:

$$0.8 f_{pu} A_{ps} \times 1.2 \times 1.5 \times 1.10 = 1.58 f_{pu} A_{ps}$$

which is very close to the $1.60 f_{pu} A_{ps}$ recommended. Therefore, the limit states recommended are not revolutionary but represent more of a world norm.

DESIGN CRITERIA

The various factors affecting the design of post-tensioned anchorage zones in Refs. 2 and 3 and the preceding discussions can now be restated in terms of specific design criteria. A complete design may follow one of two routes, namely, not to permit any cracks at all to form at service loads, or alternatively, to permit the formation of cracks at service load but limit their maximum widths. Both routes must satisfy the serviceability and ultimate limit state requirements of Eqs. (6) and (7).

CRACK FREE DESIGN

Although in some instances, such as for interior members, the formation of anchorage zone cracks at service load levels may be acceptable, for the most part they should not be tolerated for reasons of freeze-thaw durability or corrosion threats and for general aesthetics. There are two means of achieving service load level crack-free anchorage zone design:

1. Proportion the segment to remain

Table 4. Statistical Evaluation of Crack Width Data for Various Types of Tendons.

Type of tendon	$\bar{X}$ (percent)	σ (percent)	$\bar{X} - \sigma$ (percent)	$\bar{X} - 2\sigma$ (percent)
Straight tendons with spiral reinforcement	36	14	22	8
Inclined tendons with spiral reinforcement	51	26	25	0
Inclined tendons with 100 psi* lateral post-tensioning	25	5	20	15

Note: $\bar{X}$ = the mean percent increase in load above the cracking load before crack widths begin to exceed 0.013 in. (0.33 mm).
*1 psi = 0.006895 MPa.

uncracked with no dependence on supplementary anchorage zone reinforcement using Eqs. (2) and (6) while providing sufficient supplementary reinforcement to satisfy the ultimate strength requirement of Eq. (7).

2. If, due to geometric restrictions the section would not remain uncracked at the service level stressing load according to Eq. (2), then supplementary reinforcement, either active or passive, should be used to raise the cracking load to a level which satisfies the requirements of Eq. (6). The expected increase in cracking load above that given by Eq. (2) for a given geometric configuration and reinforcing scheme is given by Eq. (3). A final check must be made to satisfy the ultimate strength requirement of Eq. (7).

ACCEPTABLE CRACK DESIGN

If for some reason the requirements mentioned above cannot be met, it is possible in some cases to maintain service level crack widths within the general AASHTO-ACI acceptable levels [0.013 in. (0.33 mm)] through the use of supplementary reinforcement, particularly lateral prestressing. Due to scatter in the experimental crack width data, the assessment of allowable load increase beyond cracking load is difficult. The data shown in Table 4 were obtained from Ref. 3.

The values for the full-scale inclined tendon specimens were calculated from crack width data measured within a distance of $4a'$ (see Fig. 1) from the loaded face, thus inside the range of influence of the supplemental reinforcement. Crack widths at the point of maximum tendon curvature were generally wider at a given load, but since no supplementary reinforcement was provided at that location the results were not usable. Selection of one standard deviation below the mean values implies that with adequate spirals or lateral post-tensioning, nominal loads approximately 20 percent above the cracking loads calculated from Eq. (3) can be tolerated with acceptable crack widths.

Specimens with orthogonal supplementary reinforcement exhibited unacceptably wide cracks at first cracking and thus no increase is recommended. The more conservative use of a criterion two standard deviations below the mean would indicate that only lateral post-tensioning would give a useful increase

in allowable load beyond cracking (15 percent).

Until more extensive experimental evidence is available concerning crack width control in the anchorage zone, the above recommendations must be considered very tentative and the prudent designer should make every effort to use the more certain "no crack" design procedure above. Should a large overload occur on a section designed for no cracking, an additional buffer would be available (20 percent) before the section would experience severe cracking distress.

DESIGN OF SUPPLEMENTAL REINFORCEMENT

In order to obtain the strength increases indicated in Eqs. (3) and (4), supplementary anchorage zone reinforcement must meet certain minimum requirements.

Spiral Reinforcement

Spiral reinforcement for the anchorage zone should be proportioned to ensure that the spiral confinement is sufficient to control early cracking. The amount of spiral required can be determined from the general relation between degree of internal confinement and increase in compressive strength as proposed by Richart et al.[8]

In keeping with the general philosophy of limit state design, a strength reduction factor should be applied to the capacity carried by the confined concrete. In addition, wherever a spiral is required, an arbitrary minimum diameter of ¼ in. (6.4 mm) is suggested so that a sturdy unit which will hold its shape is furnished. Thus:

$$A_{sp} \geq \frac{f_1 - \phi\,(0.85 f'_{c_i})}{\phi\,(8.2 f_s)} Ds \geq 0.05 \text{ in.}^2 \ (32 \text{ mm}^2) \quad (8)$$

or for design:

$$A_{sp} \geq \frac{f_1 - 0.6 f'_{c_i}}{4 f_y} Ds \geq 0.05 \text{ in.}^2 \ (32 \text{ mm}^2) \quad (8a)$$

where

A_{sp} = spiral wire cross-sectional area, sq in.
f_1 = post-tensioning design load divided by area confined by spiral ($f_1 = 4P/\pi D^2$, psi)
f'_{c_i} = specified compressive strength of concrete at time of stressing, psi
D = outside diameter of spiral, in.
s = pitch of spiral, in.
f_s = allowable stress in spiral steel ($f_s = 0.7 f_y$, psi)
f_y = spiral yield strength, but not more than 60,000 psi
ϕ = 0.70 for spiral design

Note: 1 in. = 25.4 mm; 1 psi = 0.006895 MPa.

See Fig. 3a for details concerning spiral geometry.

For the design of a spiral based on Eq. (8a), the following recommendations are made:

1. The outside diameter of the completed spiral, D, should be as large as possible within the confines of the web or slab, while still satisfying cover requirements. This recommendation is limited to thin web applications where $0.05 \leq t/2a \leq 0.25$. For tendons located near the side face of thick web sections, the radius of the spiral should be the edge distance less the required cover. For tendons located in the center portions of wider webs, the spiral diameter should be the maximum linear dimension of the anchorage projected bearing surface (or approximately $2a'\sqrt{2}$ for square anchors).

2. The spiral pitch should be as small as possible, but not less than that required to readily pass the maximum aggregate size used in the concrete mix. The AASHTO Bridge Specifications[9] and the ACI Building Code[10] recommend a minimum spiral clear distance pitch of 1 in. (25.4 mm) or 1½ times the maximum aggregate size for column spirals.

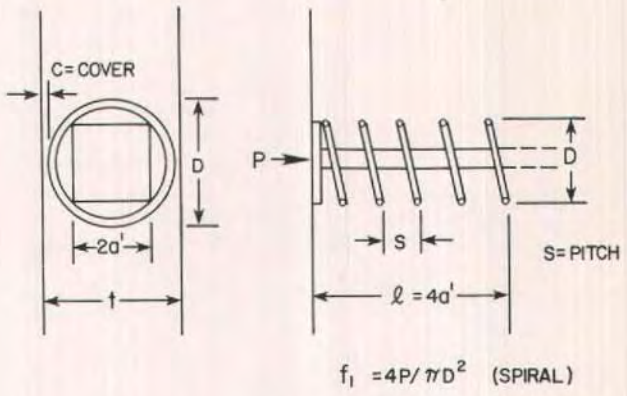

$f_l = 4P/\pi D^2$ (SPIRAL)

(a) SPIRAL

CLOSED STIRRUP

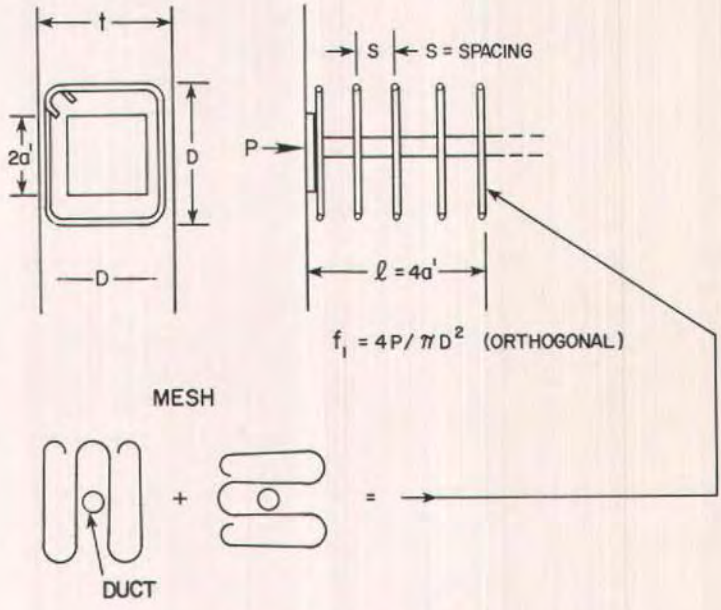

$f_l = 4P/\pi D^2$ (ORTHOGONAL)

(b) ORTHOGONAL

Fig. 3. Passive reinforcement design.

3. The spiral should begin at the anchor bearing plate and the minimum length of the spiral should be $4a'$. Longer spirals affixed to the anchor will not raise the cracking load significantly.[3] The design of spiral reinforcement in regions of tendon curvature to control cracking due to multistrand effects is discussed later.

Orthogonal Reinforcement

For passive reinforcement applications where spiral reinforcement cannot be used, an orthogonal grid of closely spaced closed stirrups or a mesh similar to that shown in Fig. 3b may be substituted. Since massive amounts of orthogonal reinforcement were shown to have little effect in preventing cracking in the anchorage zone,[3] the required reinforcement can be calculated by using the same procedure and equation presented for spiral reinforcement design above.

While this method may at first appear unconservative, since it is known that orthogonal reinforcement is substantially inferior to the spiral, the trends presented in Ref. 3 clearly show that addition of substantial reinforcement beyond that calculated by Eq. (8) is nonproductive.

The only required definition changes from those presented above are that the spiral diameter, D, becomes the minimum lateral dimension of the orthogonal closed stirrup (see Fig. 3b). The desired configurations for confinement are square closed stirrups, or better, a square mesh as shown in Fig. 3b. The s term in Eq. (8a) becomes the stirrup spacing, rather than spiral pitch. All other recommendations on placement remain the same as for the spiral.

Active Reinforcement

For full utilization of the cracking and ultimate load increases recommended in Eqs. (4) and (5), active reinforcement in the form of lateral post-tensioning (LPT) should be designed as follows:

1. LPT tendons should be placed as close as possible to the loaded face and should extend throughout the height of the web.

2. LPT load levels should be designed to produce a minimum of 100 psi (690 kPa) lateral precompression across the web section after losses. Considering the possible seating losses over the short length, initial stressing should provide between 150 and 200 psi (1035 and 1380 kPa) precompression. The lateral precompression stress can be estimated as the total lateral post-tensioning load divided by a nominal effective area (at), where a is the half height of the web and t is the web thickness (see Fig. A2).

3. LPT tendons should be placed in pairs or as U stirrups with tendons laterally equidistant from the longitudinal tendon duct to minimize lateral moments being set up in the web.

4. LPT tendons should be grouted and should utilize the most positive seating load lock-off mechanism available.

Reinforcement for Multistrand Effects

Although no tests were performed in this series to investigate the most effective control measure for multistrand cracking with curved tendons, previous model tests[11] have shown spiral reinforcement to be an efficient means of control. Until other detailed tests can be performed, the following design method should produce a conservative solution:

1. Given the internal diameter of the tendon duct and the number of strands to be used, make a scale drawing of the duct with all strands placed as close as possible to the concave side of the duct as would occur when the stressing load is applied. Draw two tangential lines from the center of the duct to the outside of the outermost strands as in Fig. 4a. This defines the loaded half angle α.

2. The radial force per unit length, p,

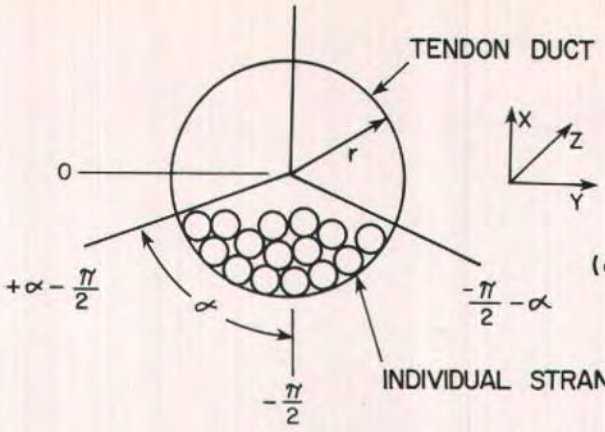

(a) GEOMETRY AT STRESSING LOAD

(b) APPROXIMATE LOADING

r = INSIDE RADIUS OF TENDON DUCT

Q = EQUIVALENT PRESSURE

$$Q = \frac{p90}{\alpha \pi r} = \frac{P90}{R \alpha \pi r}$$

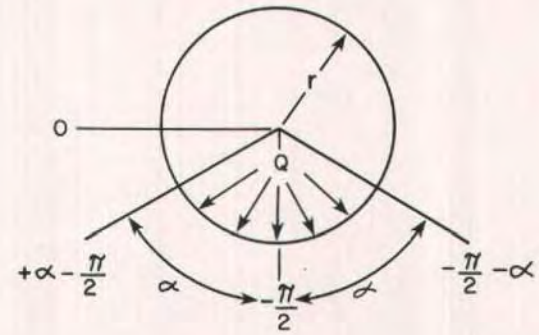

$$\text{ARC LENGTH} = 2\alpha \cdot \frac{2\pi r}{360} = \frac{\alpha \pi r}{90} \quad (\alpha \text{ in DEGREES})$$

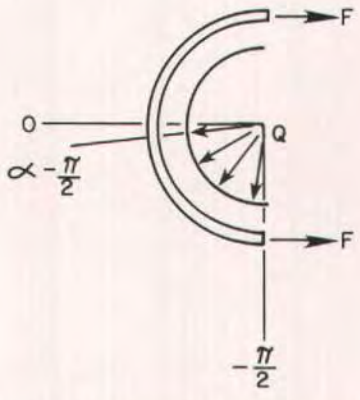

(c) EQUILIBRIUM

$\Sigma F_y = 0$

F = FORCE IN SPIRAL

Fig. 4. Spiral confinement for multistrand loading.

($p = P/R$ where P = post-tensioning load in kips, R = radius of curvature at the point of interest, in.) is assumed to be uniformly applied over the duct bearing arc length between the two lines drawn during Step 1. The quantity Q is the equivalent uniform pressure along the loaded arc segment, as illustrated in Fig. 4b.

3. The lateral force that would have to be resisted by spiral reinforcing, F, as shown in Fig. 4c, can be calculated by a simple equilibrium analysis from $\Sigma F_y = 0$ as:

$$\int_{-\pi/2}^{\alpha - \pi/2} (Qsr\, d\alpha) \cos \alpha - 2F = 0$$

$$Qsr \sin \alpha \Big]_{-\pi/2}^{\alpha - \pi/2} = 2F$$

$$Qsr\,(1 - \cos \alpha) = 2F$$

$$F = \frac{Qsr\,(1 - \cos \alpha)}{2} \qquad (9)$$

where

F = force in spiral, lbs
Q = equivalent uniform pressure along the arc segment as calculated in Step 2 [$Q = 90{,}000\,P/(R\pi\alpha r)$, psi]
P = design post-tensioning load, kips
R = minimum radius of curvature of tendon at critical location, in.
r = inside radius of tendon duct, in.
s = pitch of the spiral, in.
α = one-half the loaded arc angle, deg, but not greater than 90 deg.

If the allowable steel stress in the spiral is given by $f_s = 0.6\,f_y$ (psi), then the required rod area to be used in fabricating the spiral would be:

$$A_{sp} = \frac{F}{f_s} = \frac{Qsr(1 - \cos \alpha)}{2f_s} \qquad (10)$$

Note: 1 in. = 25.4 mm; 1 lb = 4.45 N; 1 kip 4.448 kN; 1 psi = 0.006895 MPa; 1 sq in. = 6452 mm².

Using the expression for Q above:

$$A_{sp} = \frac{45{,}000\,Ps\,(1 - \cos \alpha)}{\pi\,\alpha R f_s}$$

$$> 0.05 \text{ sq in. } (32 \text{ mm}^2) \qquad (11)$$

The amount of spiral reinforcement needed to resist the forces set up by the multistrand effect is not excessive. As an example, assume a 45-deg inclined, curved tendon with a minimum radius of curvature of 143 in. (3630 mm) and duct inside diameter of 2½ in. (63 mm) at a design load of 400 kips (1.78 MN). For α = 90 deg (tendon duct one-half full), a spiral f_s of 0.7 (60) = 42 ksi (290 MPa) (Grade 60 reinforcement) and a pitch of 2 in. (51 mm) would require a spiral rod diameter of 3/16 in. (4.8 mm).

In this case the arbitrary minimum size of a ¼ in. (6.4 mm) spiral would govern. The spiral hoop diameter, as previously mentioned, should be as large as possible while meeting the cover requirements and minimizing placement difficulties.

Spirals to control multistrand effects should be provided throughout any region where significant lateral forces may be set up. This may be conservatively estimated as regions where the nominal shear stress in the cover concrete beside the tendon duct exceeds the usual limiting shear diagonal tension stress of $2\sqrt{f'_c}$. This will occur when:

$$2F_o \geq 2\,\phi\,\sqrt{f'_{c_i}}\,(Cs) \qquad (12)$$

Where:

$2\,\phi\,\sqrt{f'_c} = 1.7\,\sqrt{f'_{c_i}}$ = nominal shear strength of concrete, psi
C = minimum concrete cover on one side of tendon duct, in.
s = spiral pitch, in.
F_o = lateral force equivalent to that resisted by one leg of a spiral, lbs

Combining Eqs. (9) and (12), the spi-

ral is required throughout those regions where:

$$F > F_o \tag{13}$$

Therefore:

$$Q \geq \frac{2\phi \sqrt{f'_{c_i}} C}{r\,(1 - \cos \alpha)} \tag{14}$$

This expression corresponds to those regions where:

$$R \leq \frac{90{,}000\,P\,(1 - \cos \alpha)}{\pi\,\alpha C\,2\,\phi \sqrt{f'_{c_i}}} \tag{15}$$

This may extend along the tendon for several web thicknesses on either side of the point of minimum radius of curvature (R). Since the designer would use the tendon force P in his calculations, Eq. (15) may be written in terms of a side face cracking load, P_o, as:

$$P_o = \frac{2\phi \sqrt{f'_{c_i}} CR\,\pi\,\alpha}{90{,}000\,(1 - \cos \alpha)} \tag{16}$$

where the minimum value of R should be used and $\phi = 0.85$.

To check the general applicability of these expressions, results of several of the full-scale tests may be examined using $\phi = 1.0$ since all properties are known. For example, Specimen FS2B had a 2.6 in. (66 mm) inside diameter duct with a 12-strand ½-in. (12.7 mm) diameter 270 ksi (1863 MPa) tendon in a 12 in. (305 mm) wide web. In Specimen FS2B the measured P_{cr} was 330 kips (1.5 MN), P_{design} was 400 kips (1.78 MN), the minimum R was 191 in. (4.58 m), α was 67.5 deg, f'_c was 4627 psi (31.9 MPa), and r = 1.25 in. (31.8 mm). Thus:

$$C = \frac{12 - 2.5}{2} = 4.75 \text{ in. (121 mm)} \tag{17}$$

From Eq. (16) with $\phi = 1.0$:

$$P_o = \frac{(2.0) \sqrt{4627}\,(4.75)\,(191)\,\pi\,(67.5)}{90{,}000\,(1 - \cos 67.5)}$$

$$= 471 \text{ kips (2.1 MN)}$$

Since P_{des} = 400 kips (1.78 MN) < P_o, no side face cracking near the point of minimum radius of curvature would be expected until after anchorage zone cracks had appeared. Similarly, use of Eq. (15) would indicate R_o to be 162 in. (4.11 m). Since the minimum R was 191 in. (4.85 m), $R > R_o$, so no supplementary spiral in the area of maximum curvature is needed. Specimen FS2B did crack in the anchorage zone at 330 kips (1.5 MN) and did not experience initial-side face distress.

For Specimen FS4A, first cracking occurred at 400 kips (1.78 MN) and was definitely due to multistrand effects. A 17-strand ½-in. (12.7 mm) diameter 270 ksi (1863 MPa) tendon was used in a 12-in. (305 mm) wide web. The original ductwork was removed to provide extra space so that r = 1.5 in. (38.1 mm), C = 4.5 in. (114 mm), α = 90 deg for this case, f'_c was 5200 psi (36 MPa) and minimum R = 178 in. (4.52 m). Thus, from Eq. (16) with $\phi = 1.0$:

$$P_o = \frac{2 \sqrt{5200}\,(4.5)\,(178)\,\pi\,(90)}{90{,}000\,(1 - \cos 90)}$$

$$= 363 \text{ kips (1.62 MN)}$$

Since P_{des} = 567 kips (2.52 MN) > P_o, initial cracking would be expected to occur in the region of maximum curvature. The 400-kip (1.78 MN) level at which the cracking actually occurred is in good agreement with P_o. Eq. (15) indicates R_o to be 278 in. (7.1 m). Since the minimum R was 178 in. (4.52 m), a spiral is required in the tendon curvature zone.

In design applications, the side face cracking limit state should be checked by using $P_{nom_{cr}}$ from Eq. (6) for P_o in Eq. (16) with $\phi = 1.0$ in that expression. In reality such a calculation is only a crude approximation. To achieve ultimate rupture, failure must occur on at least two radial planes connected to the duct. This would tend to raise the capacity.

Likewise, the use of the value $2\sqrt{f'_c}$ for the limiting shear strength of the

concrete in this type of application is a very approximate and conservative value. However, the results indicate that use of this model is reasonably consistent with test results. In view of the seriousness of this type of failure, the provision of spiral reinforcement in areas defined by Eqs. (15) and (16) is a prudent requirement pending further experimental study.

ANCHOR BEARING AREA

Both the experimental and the analytical results presented in Ref. 4 indicated that the cracking load is relatively insensitive to appreciable changes in bearing area and that bearing stress should not be the primary criterion for anchorage zone design. However, it is a useful tool in sizing anchor plates and web thicknesses. In addition, all tests in this investigation were short-term tests and did not reflect possible creep effects at extremely high stressing levels.

Comparison of the results of this study with the various specification trends indicated in Ref. 4 shows that agreement is much better when an increase in anchorage bearing is allowed for increased concrete surrounding the anchor. Thus, AASHTO should consider adoption of an expression similar to ACI and CEB-FIP. As suggested in Ref. 4, an effective bearing stress design criterion for post-tensioned anchorages is:

$$f_{b_{all}} = 0.8 f'_{c_i} \sqrt{A_2/A_1} \leq 1.33 f'_{c_i} \quad (18)$$

where

$f_{b_{all}}$ = allowable bearing stress under the anchor plate of post-tensioning tendons, psi

A_1 = bearing area of anchor plate, sq in.

A_2 = area of the anchorage surface concentric with and geometrically similar to the anchor plate, sq in.

f'_{c_i} = compressive strength of concrete at time of initial prestress, psi

SUGGESTED CODE OR SPECIFICATION REQUIREMENTS

The general design criteria and recommendations described above are difficult to reduce to simple, concise language suitable for direct inclusion in regulations such as the AASHTO Specifications or the ACI Building Code. The provisions are best expressed as general performance requirements in the Specification or Code but with accompanying commentary indicating possible ways of satisfying the performance requirements. The best advice to give a design engineer is to require prototype testing of unusual or untried anchorage configurations.

SUGGESTED CODE PROVISIONS

A.0 Notation

A_{ps} = nominal area of post-tensioning tendon, sq in.*

f_{pu} = specified tensile strength of post-tensioning tendons, ksi

where

f_b = maximum concrete bearing stress under anchor plate of post-tensioning tendons, psi

A_1 = bearing area of anchor plate, sq in.

A_2 = area of the anchorage surface concentric with and geometrically similar to the anchor plate, sq in.

f'_{c_i} = compressive strength of concrete at time of stressing, psi

*For code provisions and accompanying commentary the following SI conversions apply: 1 sq in. = 6452 mm²; 1 psi = 0.006895 MPa; 1 kip = 4.45 kN; 1 in. = 25.4 mm; 1 lb = 4.45 N.

A.1 Post-Tensioned Tendon Anchorage Zones

A.1.1 Reinforcement shall be provided where required in tendon anchorage zones to resist bursting, splitting, and spalling forces. Regions of abrupt change in section shall be adequately reinforced.

A.1.2 End blocks shall be provided where required for support bearing or for distribution of concentrated prestressing forces.

A.1.3 Post-tensioning anchorages and supporting concrete shall be designed to resist maximum jacking forces for strength of concrete at time of prestressing.

A.1.4 Post-tensioning anchorage zones shall be designed such that the minimum load producing cracking along the tendon path shall be at least equal to $1.10 f_{pu} A_{ps}$.

A.1.5 Post-tensioning anchorage zones shall be designed such that their strength shall be at least equal to 1.60 $f_{pu} A_{ps}$.

A.1.6 Supplementary anchorage zone reinforcement required for control of cracking or development of minimum strength may consist of passive reinforcement such as spirals or orthogonal closed hoops or mats. Active reinforcement such as lateral post-tensioning may be used.

A.1.7 Supplementary reinforcement such as spirals shall be provided to resist web face rupture in regions of high tendon curvature when multiple strand or parallel wire tendons are used.

A.1.8 Unless structural adequacy is demonstrated by comprehensive tests or a more comprehensive analysis, anchorage bearing stress at 1.1 $f_{pu} A_{ps}$ shall not exceed:

$$f_b = 0.8 f'_{ci} \sqrt{A_2/A_1} \leq 1.33 f'_{ci}$$

COMMENTARY

C.A.1 The general problems of anchorage of post-tensioned tendons are significantly different from the development of pretensioned reinforcement. Items concerning pretensioned element anchorage zones such as now included in AASHTO Section 1.6.15 should be put in a separate section. The last paragraph of AASHTO Section 1.6.15 also applies to control of spalling stress in post-tensioned beams.

C.A.1.1 This general performance statement alerts the user to the fact that the actual stresses around post-tensioning anchorages may differ substantially from those obtained by means of usual engineering theory of strength of materials. Consideration must be given to all factors affecting bursting, splitting, and spalling stresses. A refined strength analysis should be used whenever possible considering both the cracking and ultimate limit states. The engineer should require prototype scale testing of unusual or untried anchorage patterns or anchorage applications.

C.A.1.2 Where convenient, widening of the anchorage region to distribute the high localized forces is an effective way of reducing bursting and spalling stresses and raising the cracking and ultimate capacities. The effect of increased width is indicated in Eq. (A) in Section C.A.1.4.1.

C.A.1.3 In application of all anchorage zone design, the level of prestress applied and the concrete strength at time of application must be considered. This is particularly important with stage prestressing.

C.A.1.4 It is highly desirable that the anchorage zone remain uncracked at service levels to protect this vital area from corrosive and freeze-thaw deterioration. This can be ensured by proportioning the anchorage zone so that the cracking load is greater than any anticipated stressing load. In this proportioning the anchor zone can be designed

to remain crack free without supplementary anchorage zone reinforcement by use of Eqs. (A) through (D). The zone can be designed to remain free of surface cracks through provision of supplementary reinforcement which will raise the level of the cracking loads as indicated by Eqs. (E) through (G). The service load level specified, $1.10 f_{pu} A_{sp}$, contains allowances for jacking errors, material tolerances, and a margin of variability.

C.A.1.4.1 *Cracking Loads.* The cracking load for thin web post-tensioned sections without supplementary anchorage zone reinforcement can be determined for certain conditions from Eq. (A) [Eq. (1) in the text].

$$P_{cr_{(plate)}} = \text{See Eq. (1)} \qquad \text{(A)}$$

All variables are illustrated in Fig. A1 (Fig. 1 in text, not repeated). Limitations on the use of Eq. (A) assume:

(a) e, θ are both positive
(b) $0.05 \leq t/2a \leq 0.25$
(c) Anchors are assumed square, plate type
(d) Single tendon anchored in the web

The equation can be easily extended to some other practical applications as shown in Fig. A2 (Fig. 2 in text, not repeated). However, the cracking loads for multiple tendons in the same web must be assessed conservatively until further exploration of their behavior is carried out.

For sections which do not meet the above criteria, cracking loads can be obtained using three-dimensional finite element analysis techniques, or by comprehensive physical tests.

The cracking load can be calculated from a three-dimensional finite element computer analysis which has been calibrated to extensive physical tests. One such calibration (see Refs. 2 and 4 for details) indicates:

1. The maximum spalling strain (transverse tensile strain parallel to the loaded face) at the anchor plate edge must be calculated. For most cases this will require a detailed mesh refinement in the vicinity of the anchor plate edge following a preliminary analysis with a coarse grid. This is particularly important for inclined tendon blockouts with square corners. Anchorage zone reinforcement need not be modeled for this analysis.

2. The peak spalling strain corresponding to a load of 1 kip should be computed. The approximate cracking load (for a section without supplementary reinforcement) can be calculated as follows:

$$P_{cr} = \frac{\epsilon_{cr}}{\epsilon_{1-\text{kip(FEM)}}} \qquad \text{(B)}$$

where

P_{cr} = cracking load, kips
ϵ_{cr} = threshold cracking strain, $\mu\epsilon$
$\epsilon_{1-\text{kip(FEM)}}$ = peak spalling strain at plate edge from program with unit post-tensioning load of 1 kip

Calibration studies[4] indicate that appropriate values of ϵ_{cr} are 170 $\mu\epsilon$ for plate anchors with straight tendons and 1100 $\mu\epsilon$ for plate anchors with inclined tendons in which a right angle blockout is used.

For other than plate bearing-type anchorages, the cracking loads obtained from Eqs. (A) and (B) should be modified as follows:

Conical anchor:

$$P_{cr} = 0.61\, P_{cr_{(plate)}} \qquad \text{(C)}$$

Bell anchor:

$$P_{cr} = 1.08\, P_{cr_{(plate)}} \qquad \text{(D)}$$

These coefficients apply only when the anchorages present approximately the same projected bearing area.

In any physical tests to determine cracking loads, the conditions to be expected during construction of the actual structure must be replicated as precisely as possible. These include the effects of

tendon eccentricity, inclination, curvature, multiple tendons, and multiple strands, as well as anchor size, section width and height, and supplementary reinforcement.

C.A.1.4.2 *Effect of Reinforcement on Cracking.* Cracking loads as calculated from Eqs. (A) through (D) represent the minimum value to be expected for a section with no supplementary reinforcing in the anchorage zone. The addition of supplementary reinforcing will raise both the cracking and ultimate load. For sections provided with spiral, orthogonal, or active reinforcement designed in accordance with Section A.1.6, the cracking load can be determined as:

Spiral reinforcement:

$$P'_{cr} = (2.03 - 0.032\theta)\,P_{cr} \qquad (E)$$

Orthogonal reinforcement:

$$P'_{cr} = (1.61 - 0.019\theta)\,P_{cr} \qquad (F)$$

Active reinforcement:

$$P'_{cr} = (2.37 - 0.0372\theta)\,P_{cr} \qquad (G)$$

where

P'_{cr} = cracking load for the reinforced section, kips

θ = angle of tendon inclination, deg

P_{cr} = cracking load for the unreinforced section as calculated above, kips

C.A.1.5 The proper development of the post-tensioning force in unbonded tendons and in bonded tendons prior to completion of grouting is completely dependent on proper anchorage of the tendons. The anchorage capacity must be greater than any anticipated tendon load with a reasonable factor of safety. The capacity specified $1.60\,f_{pu}A_{sp}$ contains allowance for tendon tolerances, actual strength range rather than guaranteed minimum strength, and a margin of safety against the explosive type failure which would occur if an anchorage zone failed.

The ultimate load for sections without supplementary anchorage zone reinforcement is conservatively assumed to be equal to the cracking load. With the addition of reinforcement designed according to Section A.1.6, the ultimate load will be:

No supplementary reinforcement:

$$P_{ult} = P_{cr} \qquad (H)$$

Spiral reinforcement:

$$P_{ult} = (3.18 - 0.053\theta)\,P_{cr} \qquad (I)$$

Orthogonal reinforcement:

$$P_{ult} = (1.71 - 0.017\theta)\,P_{cr} \qquad (J)$$

Active reinforcement:

$$P_{ult} = (3.89 - 0.0640\theta) \qquad (K)$$

where

P_{ult} = ultimate load for reinforced section, kips

θ = angle of tendon inclination, deg

P_{cr} = cracking load for *unreinforced* section as calculated above

C.A.1.6 In order to obtain the strength increase indicated in Eqs. (E) through (K), supplementary anchorage zone reinforcement must meet the following minimum requirements.

C.A.1.6.1 *Spiral Reinforcement.* Spiral confinement must be adequate to resist cracking and fully develop the anchorage. To insure a sturdy unit the minimum spiral wire diameter is ¼ in. Minimum spiral area is:

$$A_{sp} \geq \frac{f_1 - 0.6f'_{c_i}}{4f_y} Ds \geq 0.05 \text{ sq in.}$$

where

A_{sp} = spiral wire cross-sectional area, sq in.

f_1 = post-tensioning load divided by the area confined by the spiral $= 4P_u/\pi D^2$, psi

f'_{c_i} = specified concrete compressive strength at time of stressing, psi

D = overall diameter of spiral, in.

s = pitch of spiral, in.

f_y = spiral yield strength, psi (but not more than 60,000 psi)

In thin webs, the spiral diameter, D, should be as large as possible while still satisfying cover requirements. In general, the spiral diameter should be the maximum linear dimension of the anchor projected bearing surface (the diagonal for square or rectangular anchor plates). Spiral pitch should be as small

as possible but must allow for concrete placement. The spiral should begin at the anchor plate and have a minimum length of twice the anchor plate depth or width, whichever is larger.

C.A.1.6.2 *Orthogonal Reinforcement.* While spiral reinforcement is usually superior to orthogonal reinforcement, in some applications an orthogonal grid of closely spaced closed stirrups or a mesh of orthogonal bars may be used. The minimum area of bars in such close stirrups or meshes should be calculated using the expression given in Section A.1.6.1 with the minimum lateral dimension of the orthogonal closed stirrup or mesh substituted for D and the stirrup spacing substituted for s.

C.A.1.6.3 *Active Reinforcement.* Lateral post-tensioning (LPT) is highly effective as active reinforcement. Such reinforcement should be designed on the following basis:

1. LPT tendons should be placed as close as possible to the loaded face and should extend throughout the height of the web.

2. LPT tendons should produce a minimum lateral precompression in the anchor zone of 100 psi after losses. Initial stressing should provide 150 to 200 psi. The nominal effective area for stress calculation should be taken as the web thickness times a length equal to half the section height.

3. LPT tendons should be placed in pairs equidistant from the tendon centerline to minimize lateral moments in the web.

4. LPT tendons should be grouted and should utilize the most positive seating load lock-off mechanism available.

C.A.1.7 *Reinforcement for Multistrand Effects.* For post-tensioning applications with significant tendon curvatures and with multiple strand tendons, a side face failure mechanism may govern the failure of the section. Any time a loaded tendon follows a curved path, normal and friction forces are set up along the length of the duct. In regions of small radius of curvature, lateral forces due to the flattening out of the multistrand tendon under stressing loads can cause tendon path cracking at loads below those which initiate cracking in the anchorage zone proper. Such cracking will be likely if:

$$P_{des} \geq P_o = \frac{2\phi\sqrt{f'_{c_i}}CR\pi\alpha}{90{,}000\,(1-\cos\alpha)}$$

or

$$R_{min} \leq R_o = \frac{90{,}000\,(1-\cos\alpha)}{\pi\alpha C 2\phi\sqrt{f'_{c_i}}}$$

where

P_{des} = P = minimum cracking design load ($1.10 f_{pu} A_{ps}$), kips
P_o = side face cracking load, kips
ϕ = strength reduction factor for shear = 0.85
f'_{c_i} = compressive strength of concrete at time of stressing, psi
C = minimum concrete cover on one side of duct, in.
R = minimum radius of curvature of tendon, in.
α = one-half the duct loaded arc angle, deg (but not more than 90 deg)

If $P_{des} \geq P_o$ or $R_{min} \leq R_o$ then supplementary reinforcement will be required in the regions where $R \leq R_o$. Since the region of minimum radius of curvature is typically some distance removed from the anchorage zone (and the benefit of the supplemental reinforcement there), additional reinforcement must be provided. This can be accomplished most efficiently through the use of spiral reinforcement designed as follows:

1. The radius of curvature along the tendon profile is calculated as:

$$R = \frac{[1 + (dx/dz)^2]^{3/2}}{|d^2x/dz^2|}$$

where x is the dependent vertical variable and z is the longitudinal variable.

Most tendon profiles can be defined by the equation:

$$x = Az^3 + Bz^2 + Cz + D$$

The minimum radius of curvature R can thus be calculated.

2. Given the internal diameter of the tendon duct and the number of strands used, make a scale drawing of the duct with all strands placed as close as possible to the concave side of the duct as would occur when the stressing load is applied. Draw two radial lines from the center of the duct, tangent to the outside of the outermost strand, as in Fig. A3 (Fig. 4 in text, not repeated). This defines α. The area of spiral required is then:

$$A_{sp} = \frac{45{,}000\,Ps\,(1 - \cos\alpha)}{\pi\alpha R\,(0.6f_y)} \geq 0.05 \text{ sq in.}$$

General spiral proportioning should follow the requirements in Section A.1.6.1. The spiral should extend throughout those regions where $R \leq R_o$ but at least $2t$ (where t = web thickness) to either side of the point of minimum radius of curvature. Such spiral reinforcement designed for multistrand cracking need not be used in areas where equivalent or stronger primary anchorage zone reinforcement has already been supplied.

C.A.1.8 *Bearing Stress.* In many cases the adequacy of anchorage assemblies will have been demonstrated by comprehensive tests or analyses. However, in other cases it is desirable to have a relatively simple method to proportion the size of bearing plates. Comprehensive tests and analyses show that the tendon anchorage cracking load is relatively insensitive to bearing area and bearing stress. However, the confinement provided by concrete surrounding the bearing plate does increase the cracking load somewhat. The value of allowable stress given in Section A.1.8 reflects recent test experience and tends to be a conservative bearing stress for use in sizing bearing plates. The expression given represents a slight liberalization over ACI 318-77 values and a substantial liberalization over current AASHTO values for anchors which do not extend fully across the web.

CONCLUSIONS

At the inception of this study the common American practice for post-tensioned anchorage zone reinforcement design was for the structural designer to specify tendon force and location and to allow the contractor to choose a post-tensioning system. Both then usually relied on the hardware supplier to furnish detailed advice on the use of the system. Often the supplier's knowledge was based on limited tests, on practical experience (generally with enlarged cast-in-place end blocks), and on the published work of such investigators as Guyon or Zeilinksi and Rowe, who relied on the classical bursting stress approach to design of supplementary anchorage zone reinforcement.

Although these designs usually worked well for straight tendon applications with little eccentricity, they were insufficient to control anchorage zone cracking in some thin member applications such as in precast segmental box girder bridge web sections. In these applications, the tendons were often not only eccentric, but also highly inclined in order to pick up a portion of the dead load shear.

Because of the highly proprietary nature of the industry, those companies which did have experience with such problems were often reticent to publish this knowledge in the public literature. American specifications such as AASHTO and the ACI Building Code were framed in very limited terms of allowable bearing stresses, and did not reflect the effects of section aspect ratio, of tendon eccentricity, curvature, and inclination, nor the effect of supplementary reinforcement.

This investigation provides a starting point for the practicing engineer to address many common thin web post-ten-

sioning applications as well as a separate check method to evaluate the recommendations of the hardware supplier. In the test program and the analytical investigations, the scope was restricted to the anchorage of single large tendons in an anchorage zone. Both the analytical and experimental study should be expanded to cover the practical case of multiple tendons anchored in close proximity which may greatly increase the cracking problem.

The results of this study reflect a composite formed from three sources. These include physical tests of approximately forty quarter-scale microconcrete models, physical tests of nine full-scale prototype concrete specimens designed to replicate post-tensioning conditions found in the web sections, and results of an extensive series of three-dimensional linear elastic finite element computer analyses.

A linear regression analysis of the experimental data yielded an empirical equation for the load causing formation of the tendon path crack in sections without supplementary anchorage zone reinforcement. This type of crack has previously been referred to as the "bursting" crack in the literature. These values were then modified by appropriate factors to yield results where reinforcement was present. The variable trends observed experimentally were in close agreement with the computer analysis results.

The empirical equation for cracking load in this study has the following limitations:

1. For inclined tendons, the eccentricity e and inclination θ must always be assumed positive.

2. Thin web sections are assumed.

$$0.05 \leq \frac{\text{Web thickness}}{\text{Section depth}} \leq 0.25$$

3. Multiple tendons anchored in the same web section are not expressly covered. The cracking load for such applications may be significantly lower.

4. The anchorage is assumed to be square. Rectangular plates with the long dimension oriented parallel to the web face can also be used. Equivalent areas of circular plates may be used.

For those applications which fall outside these limits, such as multiple tendons, solutions can be obtained from comprehensive three-dimensional finite element analysis programs such as the program PUZGAP using calibration techniques described in Ref. 4.

Major Conclusions

1. The load required to cause formation of the tendon path crack increases with increasing web width. Increasing the angle of inclination, or the eccentricity of the tendon, decreases the cracking load. The cracking load for plate-type bearing anchors with no supplementary anchorage zone reinforcement can be calculated from Eq. (1).

2. Anchor geometry can affect the cracking load. Tests using plate-, bell- and cone-type anchors indicate factors should be applied to calculated cracking loads for plate anchors as given in Eq. (2). Those values are for sections without supplementary anchorage zone reinforcement. Ultimate load for reinforced plate- and cone-type anchors occurred at loads only nominally above the cracking load. Unreinforced bell anchors exhibited ultimate failure at loads approximately 25 percent above those which cause cracking.

3. Tendon path cracks can occur at points well removed from the anchorage zone in sections where the tendon profile has significant curvature and multiple strand tendons are used. This is due to the tendency for the bundle to flatten out within the confines of the duct, thus creating lateral forces sufficiently high to cause not only cracking but side face rupture as well.

4. When using passive reinforcement, spirals exhibit much better performance than standard orthogonal reinforcement both for increasing cracking and ulti-

mate loads, and for controlling crack widths. Spiral reinforcement has the effect of changing the cracking pattern from a single tendon path crack to a series of parallel cracks which exhibit a reduction in the average crack width. The spiral advantage is greater for thinner web sections, making it the preferred choice of passive reinforcement. Design equations for the spirals are presented which are similar to those used for design of spiral column reinforcement.

5. Active reinforcement (lateral post-tensioning) is the most efficient means of controlling anchorage zone cracking. A relatively small precompression of 100 psi (0.69 MPa) across the anchorage zone of a section with an inclined, curved, multiple strand tendon raised the cracking load 33 percent above that for an unreinforced section. The optimum location for the lateral prestress is as close to the loaded face as is feasible.

6. Static, linear elastic, three-dimensional finite element analyses can be used to predict the state of stress of the anchorage zone with reasonable accuracy up to the cracking load. Calibration studies show that for straight tendons, a peak spalling tensile strain of 172 $\mu\epsilon$ near the edge of the anchorage as calculated by the program corresponds to initiation of tendon path cracking in test specimens without supplementary reinforcement. The corresponding strain for inclined tendons in which a right angle blockout is modeled is 1150 $\mu\epsilon$, due to the high stress concentration induced by the presence of the idealized corner.

REFERENCES

1. Stone, W. C., and Breen, J. E., "Behavior of Post-Tensioned Girder Anchorage Zones," PCI JOURNAL, V. 29, No. 1, January-February 1984, pp. 64-109.
2. Stone, W. C., and Breen, J. E., "Analysis of Post-Tensioned Girder Anchorage Zones," *Research Report 208-1*, Center for Transportation Research, The University of Texas at Austin, April 1981.
3. Stone, W. C., Paes-Filho, W., and Breen, J. E., "Behavior of Post-Tensioned Girder Anchorage Zones," *Research Report 208-2*, Center for Transportation Research, The University of Texas at Austin, April 1981.
4. Stone, W. C., and Breen, J. E., "Design of Post-Tensioned Girder Anchorage Zones," *Research Report 208-3F*, Center for Transportation Research, The University of Texas at Austin, June 1981.
5. Breen, J. E., Cooper, R. L., and Gallaway, T. M., "Minimizing Construction Problems in Segmentally Precast Box Girder Bridges," *Research Report 121-6F*, Center for Highway Research, The University of Texas at Austin, August 1975.
6. Berezovytch, W. N., "A Study of the Behavior of a Single Strand Post-Tensioning Anchor in Concrete Slabs," Unpublished Master's Thesis, The University of Texas at Austin, May 1970.
7. MacGregor, J. G., "Safety and Limit States Design of Reinforced Concrete," *Canadian Journal of Civil Engineering*, V. 3, No. 4, 1976.
8. Richart, R. E., Brandtzaeg, A., and Brown, R. L., "A Study of the Failure of Concrete Under Combined Compressive Stresses," University of Illinois Engineering Experiment Station Bulletin No. 185, 1928.
9. AASHTO, *Standard Specifications for Highway Bridges*, American Association of State Highway and Transportation Officials, 12th Edition, Washington, D.C., 1977.
10. ACI Committee 318, "Building Code Requirements for Reinforced Concrete and Commentary (ACI 318-77)," American Concrete Institute, Detroit, Michigan, 1977.
11. Kashima, S., and Breen, J. E., "Construction and Load Tests of a Segmental Precast Box Girder Bridge Model," *Research Report 121-5*, Center for Highway Research, The University of Texas at Austin, February 1975.

APPENDIX

EXAMPLES ILLUSTRATING DESIGN PROCEDURE

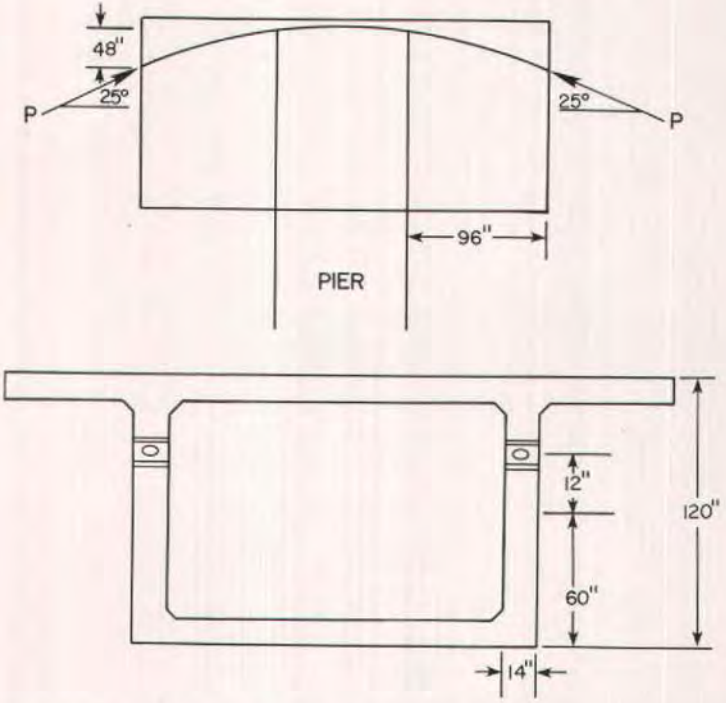

Fig. A1. Example 1 cross section and tendon profile.

EXAMPLE 1

Assume a preliminary design for a post-tensioned, segmental precast box girder bridge has developed a tendon profile and cross section as shown in Fig. A1. The maximum temporary prestress in each web section is 495 kips (2.2 MN). Also assume that the tendon has fifteen ½-in. (12.7 mm) diameter 270-ksi (1863 MPa) strands. A plate bearing-type anchor 13.25 in. (337 mm) square will be used to anchor the tendon. The compressive strength of the concrete will be 5000 psi (34.5 MPa) within tolerance levels to be expected at the precast yard.

Problem

Given the above data:

(a) Will the anchor plate satisfy the bearing stress requirements of Section A.1.8?

(b) Will the section satisfy Sections A.1.4 and A.1.5 with no supplementary reinforcement?

(c) If the answer to (b) is no
  (1) Design a reinforcing scheme that will satisfy all the requirements of Sections A.1.4 and A.1.5.
  (2) Redesign the section for no cracking with no supplemental reinforcement. Then sup-

ply a suitable passive reinforcing scheme to meet ultimate requirements.

(d) Since the tendon is curved, check to see if the section satisfies Section A.1.7 (multistrand effects). Reinforce as needed.

Solution

Available information:

$t = 14$ in. (356 mm)
$2a = 120$ in. (3050 mm)
$e = 12$ in. (305 mm)
$2a' = 13.25$ in. (337 mm)
$\theta = 25$ deg

$f_{sp} = 6.5\sqrt{f'_c} = 6.5\sqrt{5000}$
$= 460$ psi $= 0.460$ ksi (3.17 MPa)

$A_1 = (13.25)^2$
$= 176$ sq in. (113500 mm^2)

$A_2 = (14)^2 = 196$ sq in. (126400 mm^2)

$P_{nom} = 0.8 f_{pu} A_{ps} = 495$ kips (2.2 MN)
$P'_{cr} \geq 1.10 f_{pu} A_{ps} = 680$ kips (3.03 MN)
$P_u \leq 1.60 f_{pu} A_{ps} = 990$ kips (4.4 MN)

(a) Check Section A.1.8, Bearing Stress

$$f_b = \frac{1.1 f_{pu} A_{ps}}{A_1} \leq 0.8 f'_{ci}\sqrt{A_2/A_1} < 1.33 f'_{ci}$$

$$f_b = \frac{680000}{176} = 3864 \text{ psi (26.7 MPa)}$$
$$\leq (0.8)(5000)\sqrt{\frac{196}{176}}$$
$$\leq 4221 \text{ (29.1 MPa)}$$
$$\leq 6620 \text{ psi (45.7 MPa)}$$
(bearing stress ok)

(b) Check Section A.1.4, Service Level Cracking

$P'_{cr} = 1.10 f_{pu} A_{ps} = 680$ kips (3.03 MN)

From Eq. (A):

$$P_{cr} = 14\left[\frac{0.46}{24}\{38(60) - 120\} - \frac{14}{81}\{2(25) - 252(12/60)(0.46)\}\right.$$
$$\left. - \frac{103}{9}(12/60) - 7\right] + 39\,\frac{(13.25)}{2} + \frac{0.46}{5}\left\{166 - 975\left(\frac{13.25}{2(14)}\right)^2\right\} - 9.1$$
$$= 630 \text{ kips (2.8 MN)}$$

$P'_{cr} = 680$ kips (3.03 MN) $> P_{cr} = 630$ kips (2.8 MN)

Therefore, the section does not meet the cracking strength requirement of Section A.1.4.

If spiral reinforcement is provided, the new cracking load from Eq. (E) would be:

$P'_{cr} = (2.03 - 0.032\theta) P_{cr}$
$= [2.03 - 0.032(25)]\,(630)$
$= 775$ kips (3.45 MN)

This value is greater than the 680 kips (3.03 MN) required by Section A.1.4, and thus the section will not crack. This spiral reinforcement can be designed as shown later. Alternatively, from Eq. (G) active reinforcement in the form of lateral post-tensioning will also provide the necessary increase in cracking load:

$P'_{cr} = (2.37 - 0.0372\theta) P_{cr}$
$= [2.37 - 0.0372(25)]630$
$= 907$ kips (4.04 MN)

which is considerably higher than the required 680 kips (3.03 MN). Therefore, Section A.1.4 is satisfactory if either a spiral or active reinforcement is provided.

(c) Check Section A.1.5, Minimum Strength

$P_u = 1.60 f_{pu} A_{ps} = 990$ kips (4.04 MN)

To meet service load cracking requirements, either spiral reinforcement

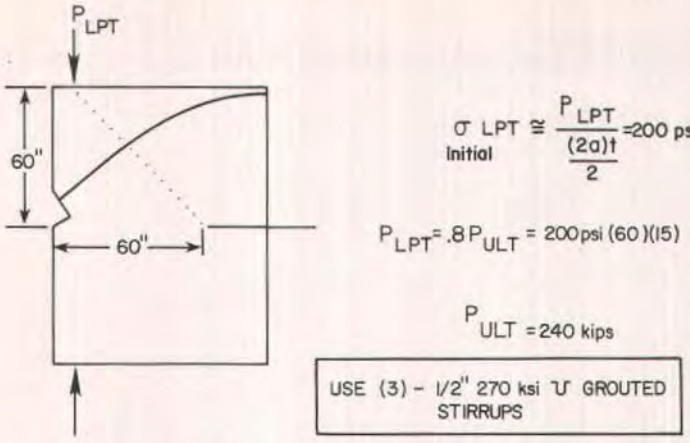

Fig. A2. Lateral post-tensioning details.

or active reinforcement is required in the section. Therefore, the minimum strength check should be made for these cases.

With spiral reinforcement, from Eq. (I):

$$P_{ult} = (3.18 - 0.053\theta)\, P_{cr}$$
$$= [3.18 - (0.053)\,(25)]\,(630)$$
$$= 1169 \text{ kips } (5.2 \text{ MN})$$

$$P_u = 990 \text{ kips } (4.04 \text{ MN}) \leq 1169 \text{ kips } (5.2 \text{ MN}) \text{ (ok)}$$

With active reinforcement, from Eq. (K):

$$P_{ult} = (3.89 - 0.064\theta)\, P_{cr}$$
$$= [3.89 - (0.064)\,(25)]\,(630)$$
$$= 1443 \text{ kips } (6.42 \text{ MN}) \text{ (ok)}$$

Either type of reinforcement must be provided to allow the section to satisfy Section A.1.5.

(d) Proportion active reinforcement to satisfy Section A.1.6.3.

The recommended minimum initial lateral precompression of 150 to 200 psi (0.69 to 1.38 MPa) across the web can be achieved by:

$$0.200 \text{ ksi} = \frac{0.8\, f_{pu} A_{ps}}{ta} = \frac{0.8(270)\, A_{ps}}{(16)(60)}$$

$$A_{ps} = 0.888 \text{ sq in. } (573 \text{ mm}^2)$$

The required area A_{ps} (LPT) can be provided by three sets of ½-in. 270-ksi U stirrups with grouted tendons placed so that the resultant load will act as close as possible to the primary load face as shown in Fig. A2.

(e) As an alternate solution to Part (d), proportion the spiral reinforcement to meet Section A.1.6.1.

From Commentary Section A.1.6.1:

$$A_{sp} \geq \frac{f_1 - 0.6 f'_c}{4 f_y} Ds$$

= cross-sectional area of bar used to fabricate spiral
$\geq$ 0.05 sq in. (32 mm²)

where

$$f_1 = \frac{4 P_u}{\pi D^2}$$
$$= \frac{(4)(990)}{\pi (13)^2}$$
$$= 7460 \text{ psi } (51.5 \text{ MPa})$$

f'_c = 5000 psi (34.5 MPa)
D = 9 in. (229 mm)
s = 2 in. (51 mm) pitch

$$A_{sp} = \frac{7460 - 0.6(5000)}{(5)(60000)} (9)(2.0)$$
$$= 0.27 \text{ sq in. } (170 \text{ mm}^2)$$

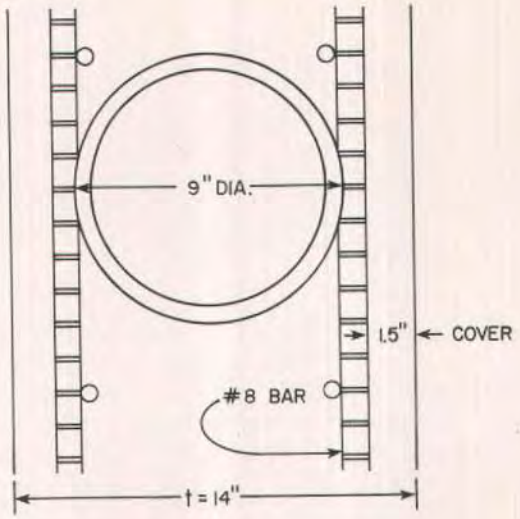

Fig. A3. Sizing spiral diameter.

$$d_{bar} = \sqrt{\frac{4\,(0.27)}{\pi}} = 0.58 \text{ in. } (14.7 \text{ mm})$$

Use ⅝ in. (16 mm) diameter 60 ksi (414 MPa) smooth rod spiral 9 in. (230 mm) overall diameter, at 2-in. (51 mm) pitch. The length of the spiral should be $4a' = 27$ in. (685 mm). The details are as shown in Fig. A3.

(f) Check Section A.1.7, Multistrand Effects

The tendon profile shown in Fig. A4 can be described by the following equation:

$$x = x_2 - A(z_2 - z)^3 - B(z_2 - z)^2$$

where the boundary conditions are assumed to be:

At x_1 $\theta = 0.436$ radians (25 deg)
$x = x_1 = 72$ in. (1.83 m)
$z = z_1 = 0$ in.

At x_2 $\theta = 0.0$ radians
$x = s_2 = 114$ in. (2.89 m)
$z = z_2 = 96$ in. (2.44 m)

Based upon these assumptions:

$$A = \frac{-2(x_2 - x_1)}{(z_2 - z_1)^3} + \frac{\theta}{(x_2 - z_1)^2}$$

$$B = \frac{3(s_2 - x_1)}{(z_2 - z_1)^2} - \frac{\theta}{(z_2 - z_1)}$$

For this problem:

$A = -4.75\,(10)^{-5}$
$B = 9.13\,(10)^{-3}$

Substituting these values into the tendon profile equation and differentiating yields:

$$x' = -1.425(10)^{-4}(96 - z)^2 + 1.826(10)^{-3}(96 - z)$$
$$x'' = 2.85(10)^{-4}(96 - z) - 1.826(10)^{-3}$$

The radius of curvature is given by:

$$R = \frac{[1 + \{-1.425(10)^{-4}(96 - z)^2 + 1.826(10)^{-3}(96 - z)\}^2]^{1.5}}{|2.85(10)^{-4}(96 - z) - 1.826(10)^{-3}|}$$

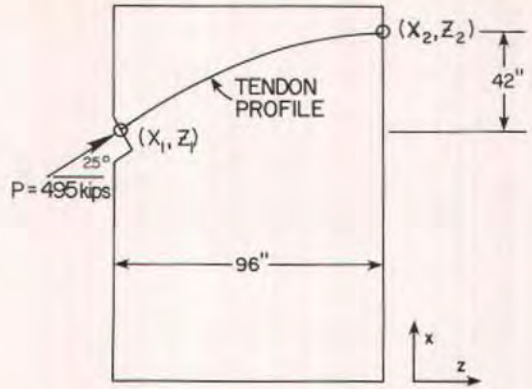

Z (in.)	R (in.)	$p = P/R$ (lb per in.)	$Q = p/20r$ (psi)
0	136.1	5319	1231
10	106.8	6779	1568
20	89.7	8071	1867
30	82.3	8497	1965
35	81.9	8840	2045
40	83.7	8649	2001
50	94.98	7621	1763
60	121	5983	1384
70	179.7	4022	930
80	366	1978	457
90	547	1323	306

Note: 1 in. = 25.4 mm; 1 lb per in. = 180.6 kg per m; 1 psi = 0.006895 MPa.

Fig. A4. Data for design of spiral reinforcement to resist multistrand cracking.

These values are tabulated in Fig. A4. A survey of these values shows that the minimum radius of curvature is 81.9 in. (2080 mm) at which point Q is calculated to be 2045 psi (14.1 MPa) for a tendon duct with a diameter of 2.75 in. (70 mm) (the recommended flexible duct for a 15-strand commercial anchor). This minimum value of R can be checked against the expression for R_o in Section C.A.1.7:

$$R_o = \frac{90{,}000P\,(1 - \cos\alpha)}{\pi\alpha C 2\phi\sqrt{f'_{ci}}}$$

For 15 strands the duct will be half full so $\alpha = 90$ deg and:

$$C = \tfrac{1}{2}\,(14 - 2.75) = 5.625 \text{ in. (143 mm)}$$

Thus:

$$R_o = \frac{(90{,}000)\,(680)\,(1 - \cos 90)}{\pi\,(90)\,(5.625)\,(1.7)\sqrt{5000}}$$
$$= 320 \text{ in. (8.13 m)}$$

Therefore, the spiral to resist multistrand effects is required wherever the curvature radius is less than 320 in. (8.13 m). From Fig. A4 it can be seen that a confining spiral for approximately 78 in. (2 m) in horizontal projection extending from the anchor over 80 percent of the curved zone is required.

The spiral area is given by:

$$A_{sp} = \frac{45{,}000Ps\,(1 - \cos\alpha)}{\pi\alpha R 0.6 f_y}$$
$$\geq 0.05 \text{ sq in. (32 mm}^2\text{)}$$

$$A_{sp} = \frac{(45{,}000)\,(680)\,(1\tfrac{1}{2})\,(1 - \cos 90)}{\pi(90)\,(82)\,(0.6)\,(60000)}$$
$$= 0.054 \text{ sq in. } (35 \text{ mm}^2)$$

Thus, a ¼-in. (6.4 mm) diameter spiral rod with a pitch of 1½-in. (38.1 mm) and an overall diameter of 9 in. (229 mm) should be used.

EXAMPLE 2

Determine the web thickness required for the box girder in Example 1 if no supplementary reinforcement is to be provided in the anchorage zone at cracking load levels. Determine if supplementary anchorage zone reinforcement is required at ultimate strength levels.

In Example 1 the design cracking load to meet Section A.1.4 was 680 kips (3.03 MN). The original box girder with 14 in. (356 mm) webs had P_{cr} = 630 kips (2.8 MN) from Eq. (A). Thus, the cracking load has to be raised (680/630 = 1.08) about 8 percent to satisfy this requirement with no supplementary reinforcement.

Of the three major geometric variables (inclination, eccentricity, and cover), the most practical and most effective change in the cracking load can be achieved through modification of web thickness. Since the ultimate capacity of a section with no supplementary reinforcement as indicated by Eq. (H) is the same as the cracking load, it is apparent that a section designed to just satisfy the cracking load requirement [680 kips (13.03 MN)] will not meet the ultimate requirements [990 kips (4.4 MN)] without additional confining reinforcement.

Assume that in this case the required increase (990/630 = 1.57) of 57 percent is considered excessive to handle by web thickening. The designer decides to increase the web width to control cracking without relying on confinement, but to provide confinement for ultimate.

On this basis, an approximate web width is selected for trial as 110 percent t = (1.10) (14) = 15.4 in. (390 mm). Thus, t = 16 in. (406 mm) is selected as a practical dimension. Eq. (A) is now checked for the new cracking load:

t = 16 in. (406 mm)
$2a$ = 120 in. (305 mm)
e = 12 in. (305 mm)
P_{nom} = 495 kips (2.2 MN)
$1.10 f_{pu} A_{ps}$ = 680 kips (3.03 MN)
$1.60 f_{pu} A_{ps}$ = 990 kips (4.4 MN)
$2a'$ = 13.25 in. (337 mm)
θ = 25 deg
f_{sp} = 0.46 ksi (3.17 MPa)
A_1 = 176 sq in. (113500 mm²)
A_2 = 256 sq in. (165200 mm²)

$$P_{cr} = \left[16 \frac{0.46}{24} [(38)\,(60) - 120] - \frac{16}{81} \left\{ (2)\,(25) - (252) \frac{(12)}{(60)} (0.46) \right\} \right.$$
$$\left. - \frac{103}{9} \frac{(12)}{(60)} - 7 \right] + (39) \quad \frac{(13.25)}{2} + \frac{0.46}{5} \left[166 - 975 \left\{ \frac{13.25}{(2)\,(16)} \right\}^2 \right] - 9.1$$
$$= 669 \text{ kips } (2.98 \text{ MN})$$

This value is still less than the 680 kips (3.03 MN) required although it is close. The next practical increase would use a web width t of 18 in. (457 mm). Rechecking Eq. (A) for t = 18 in. yields P_{cr} = 712 kips (3.17 MN) which satisfies the requirement:

P_{cr} = 712 kips (3.17 MN)
$\geq 1.10 f_{pu} A_{ps}$ = 680 kips (3.03 MN)

However, with no supplementary reinforcement the section does not satisfy the ultimate load requirement of $1.60 f_{pu} A_{ps}$. Further widening of the webs to meet this requirement would probably result in webs over 2 ft (0.61 m) wide so it is necessary to include confining reinforcement for satisfying the ultimate conditions. This indicates

that most sections will require such confinement so that it might as well be considered for crack control. Using Eq. (I) for spiral reinforcement:

$$P_{ult} = (3.18 - 0.053\theta) P_{cr}$$
$$= [3.18 - (0.053)(25)] 712$$
$$= 1321 \text{ kips } (5.88 \text{ MN})$$

This more than satisfies the requirement:

$$P_{ult} = 1321 \text{ kips } (5.88 \text{ MN})$$
$$\geq 1.60 f_{pu} A_{ps}$$
$$= 990 \text{ kips } (4.4 \text{ MN})$$

For a web width of 18 in. (457 mm) a maximum spiral diameter D of 13 in. (330 mm) can be used. Rechecking the spiral equation:

$$A_{sp} = \frac{(f_l - 0.6 f'_{c_i})}{4 f_y} Ds$$

$$A_{sp} \geq \frac{[7460 - 0.6(5000)]}{(4)(60000)} (13)(2.0)$$
$$= 0.48 \text{ sq in. } (311 \text{ mm}^2)$$
$$> 0.05 \text{ sq in. } (32 \text{ mm}^2)$$

Thus, a ¾-in. (19 mm) diameter rod at a pitch of 2 in. (51 mm) would be required. The larger diameter of 13 in. (330 mm) results in a slightly heavier spiral than in Example 1. Bearing stress would not be a problem for this wider web.

Side face multistrand effect confining reinforcement should be rechecked because of the greater side face cover thickness.

Checking R_o for the new cover:

$$C = ½ (18 - 2.75)$$
$$= 7.625 \text{ in. } (194 \text{ mm})$$

$$R_o = \frac{(90{,}000)(680)(1 - \cos 90)}{\pi (90)(7.625)(1.7)\sqrt{5000}}$$
$$= 236 \text{ in. } (6000 \text{ mm})$$

Since the minimum R is 82 in. (2080 mm), a confining spiral is still required. The expression for spiral area is not affected by the cover so a ¼-in. (6.4 mm) diameter spiral rod with a pitch of 1½ in. (38 mm) and an overall diameter of 9 in. (229 mm) should be used along the tendon path for approximately 75 in. (1.9 m) in the horizontal direction.

NOTATION

$2a$	= section height, in.
$2a'$	= width of anchor plate (assumed square), in.
A_1	= bearing area of anchor plate, sq in.
A_2	= area of anchorage surface concentric with and geometrically similar to anchor plate, sq in.
A_{ps}	= nominal area of post-tensioning tendon, sq in.
A_{sp}	= spiral wire cross-sectional area, sq in.
C	= cover, in.
D	= outside diameter of spiral, in.
e	= tendon eccentricity, in.
f_l	= post-tensioning design load divided by area confined by spiral, psi
f_b	= maximum bearing stress under anchor plate of post-tensioning tendons, psi
$f_{b_{all}}$	= allowable bearing stress under anchor plate of post-tensioning tendons, psi
f'_c	= compressive strength of concrete, psi
f'_{c_i}	= compressive strength of concrete at time of stressing, psi
f_{pu}	= specified tensile strength of post-tensioning tendons, ksi
f_s	= allowable stress in spiral steel = $0.7 f_y$, psi
f_{sp}	= split cylinder tensile strength, ksi

f_y = spiral yield strength, but not more than 60,000 psi
F = force in spiral, lbs
F_o = lateral force equivalent to that resisted by one leg of a spiral, lbs
LF = load factor representing a factor of safety against reaching a particular limit state
LPT = lateral post-tensioning
p = normal force on tendon duct, kips per in.
P = design post-tensioning load, kips
P_{cr} = cracking load, kips
P'_{cr} = predicted cracking load with supplemental reinforcement, kips
$P_{cr\,(plate)}$ = cracking load for section with plate anchor, but without supplementary reinforcement, kips
P_{LS} = best estimate of highest load to come onto structure at particular limit state
$P_{nom_{LS}}$ = best estimate of nominal strength of structure with respect to a particular limit state
P_o = side-face cracking load, kips
P_{ult} = ultimate load with supplemental reinforcement, kips
Q = equivalent pressure, psi
r = inside radius of tendon duct, in.
R = minimum radius of curvature of tendon at critical location, in.
R_o = critical radius of curvature, in.
s = pitch of spiral, in.
t = section thickness, in.
x = vertical direction
z = horizontal direction
α = one-half the loaded arc angle, deg (but not greater than 90 deg)
ϵ_{cr} = threshold cracking strain ($\mu\epsilon$)
$\epsilon_{1.kip\ (FEM)}$ = peak spalling strain at plate edge computed from finite element analysis program for unit post-tensioning load of 1 kip
θ = angle of tendon inclination (deg)
ϕ = strength reduction factor

ACKNOWLEDGMENT

This paper is based on results of Research Project 208 "Design Criteria for Post-Tensioned Anchorage Zone Bursting Stresses," conducted for the Texas Department of Highways and Public Transportation in cooperation with the Federal Highway Administration by the University of Texas at Austin Center for Transportation Research at the Phil M. Ferguson Structural Engineering Laboratory. The contents of this paper reflect the views of the authors and do not necessarily reflect the views or policies of the sponsoring agencies.

* * *

NOTE: Discussion of this paper, alone or in conjunction with the companion paper published in the January-February 1984 PCI JOURNAL, is invited. Please submit your discussion to PCI Headquarters by November 1, 1984.